International Journal of Nanoelectronics and Materials
Volume 14 (Special Issue) December 2021 [79-85]

The Design and Analysis of High Q Factor Film Bulk Acoustic Wave Resonator for Filter in Super High Frequency

N.I.M. Nor[1,2*], N. Khalid[1,2], N A Hashim[1], S. Kasjoo[1,2], Z. Sauli[1], Lam Hok Lang[1] and Chow Shi Qi[1]

[1] Faculty of Electronic Engineering Technology, Universiti Malaysia Perlis (UniMAP), Perlis, Malaysia
[2] Micro- & Nanoelectronic Research Group, Universiti Malaysia Perlis (UniMAP), Perlis, Malaysia

ABSTRACT

Filtering process is one of the highlighted issues when the operating frequency is up to medium or high GHz range in wireless transceiver system. The development of high performance, small size, filter on chip operating in GHz frequency range is the requirement of present and future wireless transceiver systems. The conventional frequency bands, below 6 GHz are already congested, thus, to satisfy this demand, the research into transceiver systems working at frequencies higher than 6 GHz has been growing. Therefore, this work proposed the design and optimization of film bulk acoustic wave resonator (FBAR) operating in frequency 7 GHz to 10 GHz with high quality (Q) factor. The effect of using different geometrical parameters to achieve high Q factor FBAR in these frequency bands is analysed. The designed FBAR achieved Q factor of 1767 at 7 GHz and 1237 at 10 GHz by using aluminium nitride as the piezoelectric thin film and molybdenum as the electrode.

Keywords: film bulk acoustic wave resonator, quality factor, high frequency

1. INTRODUCTION

The emergence of next-generation wireless data communication has motivated the development of wireless transceiver system that operates at super-high frequency (SHF) range (3 to 30 GHz). Filtering process is one of the highlighted issues when the operating frequency is up to these frequency ranges in wireless transceiver system. Therefore, development of high- performance filters that offer low loss, wide bandwidth and steep skirt and fully integrated on-chip working at SHF is growing. Filter based on film bulk acoustic wave resonator (FBAR) has been widely as it provides a higher performance over conventional bulk acoustic wave (BAW) and surface acoustic wave (SAW) resonators in the 5G technologies. However, the conventional frequency bands, below 6 GHz are already congested, thus, to satisfy this demand, the research into transceiver systems working at frequencies higher than 6 GHz has been growing. Therefore, this work is focusing on designing the FBAR operating in frequency 7 GHz to 10 GHz with high quality (Q) factor.

An FBAR comprises of a piezoelectric thin film that is sandwiched between two electrode layers as shown in Figure 1 [1]. The selection of piezoelectric material is important while designing an FBAR as it is highly related to the performance of an FBAR. The commonly used piezoelectric materials in FBAR are zinc oxide (ZnO), lithium niobate ($LiNbO_3$), lithium tantalate ($LiTaO_3$), aluminium nitride (AlN) and scandium aluminium nitride (ScAlN) [2][3][4][5]. These materials had shown good performance in FBAR applications at frequencies ranges from 4 GHz to 6 GHz due to their high acoustic velocity and electromechanical coupling coefficient. As for electrode materials, most FBAR applications require metal electrodes that have high acoustic stiffness, high acoustic impedance, low electrical resistance, compatibility with standard manufacturing techniques and a suitable surface to align the piezoelectric layer such as aluminium (Al), molybdenum (Mo), ruthenium (Ru) and platinum (Pt)[6][7].

*izza@unimap.edu.my

The important characteristics of an FBAR are the input electrical impedance (Z_{in}), electromechanical coupling coefficient (k^2_{eff}) and Q factor. The Z_{in} of an FBAR is characterised by two resonant frequencies, series frequency (f_s) and parallel frequency (f_p) where the magnitude of the electrical impedance is minimum and maximum respectively as depicted in Figure 2.

The figure also shows that the phase between resonant frequencies is 90° behaving as an inductor, while outside these frequencies, it is -90° with pure capacitive behaviour. The magnitude of impedance is minimum at f_s and maximum at f_p which are defined as Z_s and Z_p respectively. The electromechanical coupling coefficient (k^2_{eff}) is crucial when designing the FBAR as the bandwidth of FBAR filter is determined by this parameter. The electromechanical coupling coefficient can be measured as the relative difference of f_s and f_p which depends on both the material coupling factor and the resonator geometry. Quality (Q) factor is a measure of the loss of a resonant circuit and is defined as the ratio of the stored energy divided by the power dissipated in that network over one cycle. Some of the causes of losses in FBARs are electrical resistivity of the electrodes, acoustic leaks, substrate conductivity and acoustic propagation losses. The Q factor of and FBAR is defined as a function of the frequency, therefore, the Q factors are defined both at the f_s which is identified as Q_s; and at the f_p which is defined as Q_p.

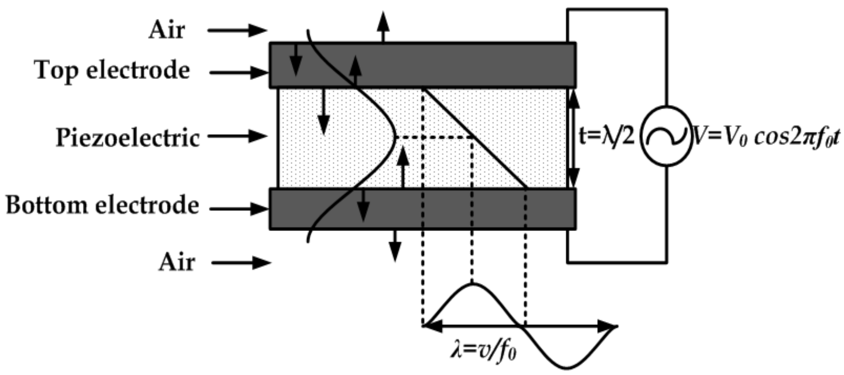

Figure 1. Bulk Acoustic Wave Propagation in FBAR [1].

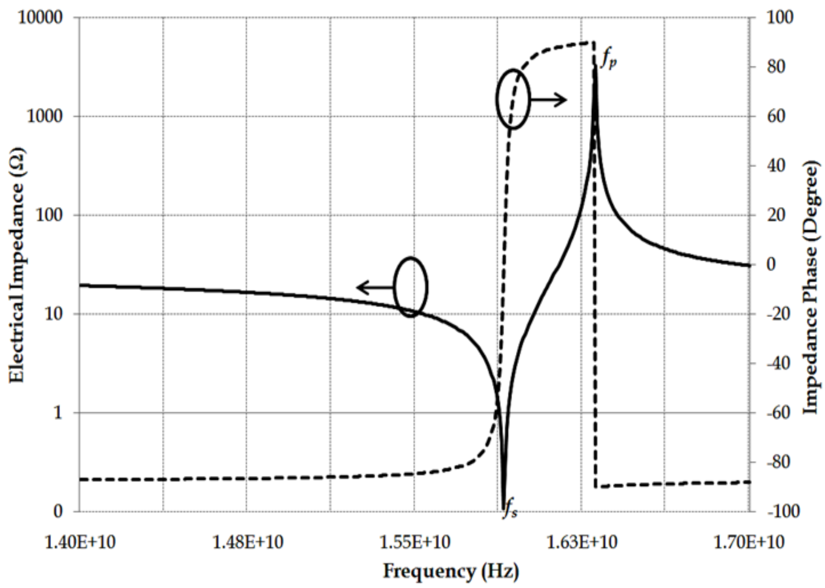

Figure 2. Characteristic of Input Electrical Impedance of FBAR

2. METHODOLOGY

The resonance frequency of the FBAR is determined by the thickness of the piezoelectric film thickness. When an electric field is produced between the electrodes, the structure is deformed by way of the inverse piezoelectric effect and launch an acoustic wave, also known as resonant standing wave [8]. These waves are produced in a frequency where a single wavelength is twice the piezoelectric film thickness. The half-wavelength is equal to the total thickness of the piezoelectric film, as depicted in Figure 1. The resonance frequency of FBAR that operate in the longitudinal mode, it is mainly determined by the thickness, t of the piezoelectric layer as given in Equation 1 [9]:

$$\theta = \frac{2\pi f_0 t}{\nu_L} \quad (1)$$

where θ is the phase, f_0 is the frequency of the acoustic wave, t is the thickness of the piezoelectric thin film and ν_L represents velocity of the acoustic wave.

The parameters used to design the FBARs in this work are as tabulated in Table 1. Three FBARs are designed for each resonance frequency with different area sizes (width x length) to analyse the effect on the performance of the FBAR in terms of electrical input impedance, electromechanical coupling coefficient and quality factor. Aluminium nitride (AlN) is chosen as the piezoelectric material and the thickness of the AlN is calculated by using Equation 1. Meanwhile, molybdenum (Mo) is selected as the electrode layers, both as top and bottom electrodes. The thickness of these electrodes is defined by the thickness ratio of 0.10 of electrode layer to piezoelectric layer. This ratio has shown highest performance as mentioned in. AlN and Mo are chosen due to their excellent material properties in designing FBARs at higher frequency as proved in [9]. There are several 1-dimensonal (1-D) modelling have been widely used in designing FBAR as mentioned in [10]. In this work, the Mason model is selected to design and analyse the important characteristics of the FBAR. The Mason model has been widely used in deriving solutions for the wave propagation through the acoustic layer by using the network theory approach. The methods to determine the electrical input impedance, electromechanical coupling coefficient and quality factor of the FBAR are detailed out in Subsection 2.1 to 2.3.

Table 1 Design Parameters of FBARs

Frequency (GHz)	**Area (μm^2)**	**Electrode Thickness (μm)**	**Piezoelectric Thickness (μm)**
7	15 × 15	0.074	0.74
	20 × 20	0.074	0.74
	25 × 25	0.074	0.74
	30 × 30	0.074	0.74
8	15 × 15	0.068	0.68
	20 × 20	0.068	0.68
	25 × 25	0.068	0.68
	30 × 30	0.068	0.68
9	15 × 15	0.058	0.58
	20 × 20	0.058	0.58
	25 × 25	0.058	0.58
	30 × 30	0.058	0.58
10	15 × 15	0.052	0.52
	20 × 20	0.052	0.52
	25 × 25	0.052	0.52
	30 × 30	0.052	0.52

2.1 Electrical input impedance (Z_{in})

An FBAR comprises with many layers as shown in Figure 3. The mass loading effects are related to the deposition of metal electrodes on the piezoelectric layer. These effects can be associated with resonance frequency shifting, which are also known as inertial effects, with the concept of energy trapping, and with the stress in the structure. The Z_{in} of the piezoelectric layer between two parallel electrodes is given in [1] as:

$$Z_{in} = \frac{1}{j\omega C_0} \times \left(1 - k_{eff}^2 \frac{\tan\theta}{\theta} \frac{(z_T+z_B)\cos^2\theta + j\sin 2\theta}{(z_T+z_B)\cos 2\theta + j(z_T+z_B+1)\sin 2\theta}\right) \quad (2)$$

where Z_T and Z_B are normalized acoustic impedance at the piezoelectric layer boundaries. θ is the half phase across the piezoelectric plate where θ=k x t and k=ω/ν_L. The boundary impedances, Z_T and Z_B are determined by the acoustic impedance matching between piezoelectric layer and electrodes. The values of Z_T and Z_B can be determined by Equation 3:

$$Z_{T/B} = Z_0^{T/B} \times \left(\frac{Z_{load}\cos\theta_{T/B} + jZ_0^{T/B}\sin\theta_{T/B}}{Z_0^{T/B}\cos\theta_{T/B} + jZ_{load}\sin\theta_{T/B}}\right) \quad (3)$$

where $Z_0^{T/B}$ is the acoustic impedance of either bottom (B) or top (T) electrode layers. Z_0 is denoted as:

$$Z_0 = A\rho\upsilon_L \quad (4)$$

where A is the area, ρ is the density, and ν_L is the longitudinal acoustic wave velocity. Z_{load} is the input load impedance seen by either the top or the bottom electrode layers, and $\theta_{T/B}$ is the acoustic-wave phase across either the top or the bottom electrode layers.

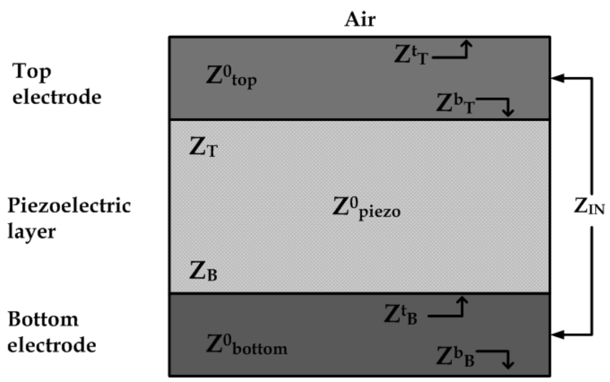

Figure 3. Equivalent of acoustic impedances of FBAR[1].

2.2 Electromechanical coupling coefficient (k^2_{eff})

As mentioned earlier, the electromechanical coupling coefficient can be measured as the relative difference of f_s and f_p. The f_s and f_p are extracted from the characteristics of the Z_{in} as previously shown in Figure 2. Therefore, the k^2_{eff} can be determined by using Equation 5 given as:

$$k_{eff}^2 = \left(\frac{\pi^2}{4}\right)\left(\frac{f_p - f_s}{f_p}\right) \quad (5)$$

2.3 Quality (Q) factor

Once the Z_{in}, f_s and f_p are determined, the Q factor can be calculated based on Butterworth Van Dyke (BVD) model mentioned in [10] by using Equation 6:

$$Q_{s/p} = \frac{f_{s/p}}{2}\left[\frac{d\angle Z_{in}}{df}\right]_{f_s/f_p} \tag{6}$$

3. RESULTS AND DISCUSSION

3.1 Influence of area size on input electrical impedance (Z_{in})

As mentioned earlier, the area size is varied to observe the influence on the electrical input impedance. Equation 2 is used to compute the electrical impedance in the resonance frequency from 7 GHz to 10 GHz. Based on the results depicted in Figure 4, it is observed that when the electrode area increases, the Z_{in} decreases for each resonance frequency. For example, at 7 GHz, with area of 15 × 15 μm², Z_{in} of 0.625 Ω is obtained. Meanwhile with area of 30 × 30 μm², Z_{in} of 0.024 Ω is achieved. Therefore, by designing an appropriate resonance area, impedance matching of the FBAR can be achieved as stated in Subsection 2.1. From the results too, it is also observed that as the frequency increases, the Z_{in} decreases too. This due to thinner AlN and Mo used in higher resonance frequencies.

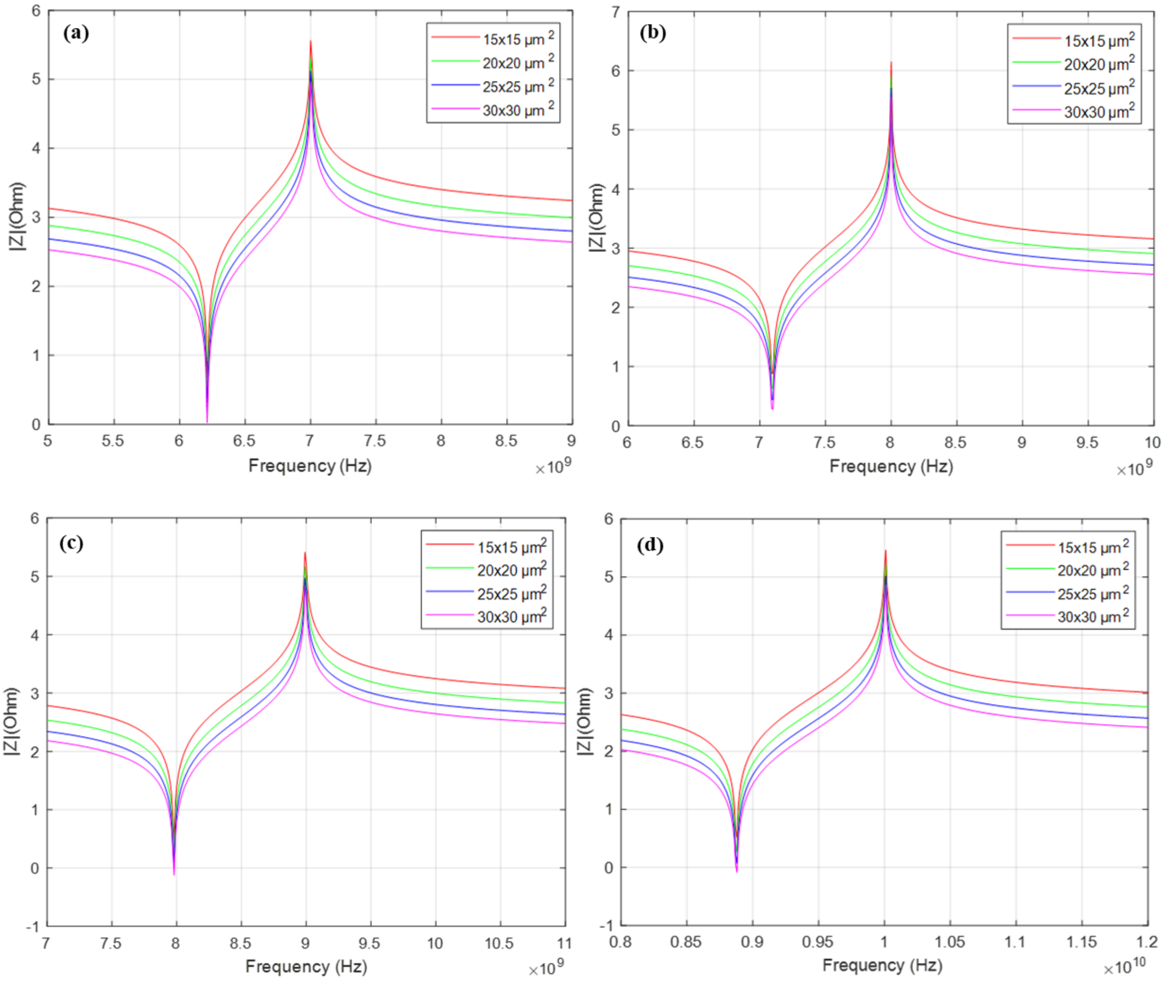

Figure 4. Influence of area size on electrical input impedance at different frequencies (a) 7 GHz (b) 8 GHz (c) 9 GHz (d) 10 GHz

3.2 Influence of area size on electromechanical coupling coefficient (k^2_{eff})

As mentioned earlier, the electromechanical coupling coefficient (k^2_{eff}) is an important parameter when designing a filter based on FBAR as it determines the bandwidth of the filter. Figure 5 shows the influence of the area size on the k^2_{eff}. Equation 5 is used to compute the values of the k^2_{eff}. From the outcomes attained in Figure 5, it can conclude that different area sizes will not affect the value of the k^2_{eff} for FBAR at the same resonance frequency. This is due to the same piezoelectric thin film and electrode materials used to design the FBAR. However, it is observed that the value of k^2_{eff} slightly decreases as the frequency increases. This is true according to the relationship given in Equation 5 which the higher the resonance frequency, the higher the k^2_{eff}.

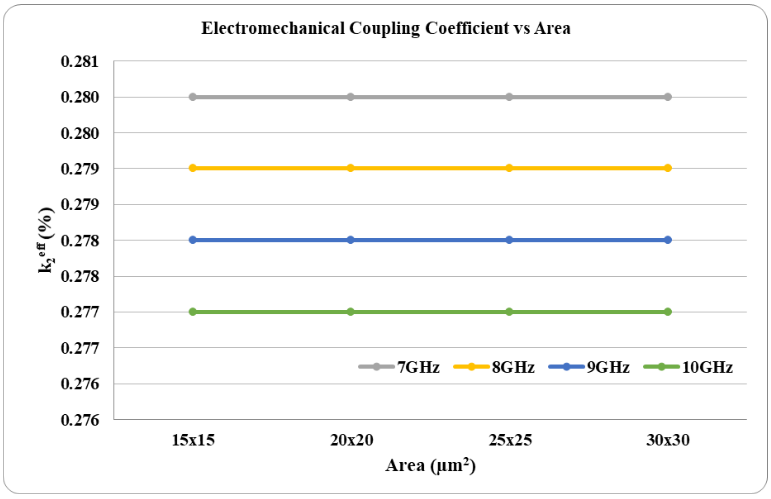

Figure 5. Influence of area size on electromechanical coupling coefficient

3.3 Influence of area size on quality (Q) factor

The influence of area size on Q factor of the FBAR is depicted in Figure 6. Equation 6 is used to calculate the Q factor. From the figure, it is observed that the Q factor has no significant effect as the area size varies for the same resonance frequency. On the other hand, it is seen that the Q factor decreases as the frequency increases. This is true according to the relationship given in Equation 6 and the results achieved in Subsection 2.1. The highest Q factor obtained is 1767at 7 GHz and 1237 at 10 GHz. Q factor is an important parameter in filter applications as it determines the insertion loss of the filter.

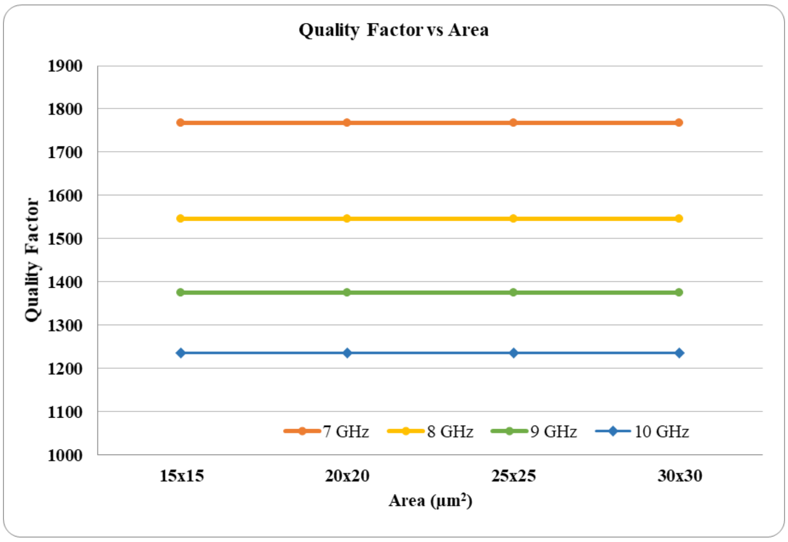

Figure 6. Influence of area size on quality factor

4. CONCLUSION

This work has successfully designed and analysed FBAR working at 7 GHz to 10 GHz by using 1-D modelling. The results obtained shows that it is possible to design FBAR with high Q factor at these frequency ranges. The results also shows that the area size has significant effect on the electrical input impedance. As the area size increases, the electrical input impedance decreases. On the other hand, the area size has no significant effect on the electromechanical coupling coefficient and quality factor of the FBAR. Future works on designing the FBAR by using 3-D finite element method (FEM) is devoted to further optimise and analyse the performance of the FBAR. The optimised 3-D FEM results can be implemented to design an FBAR filter at frequencies of 7 GHz to 10 GHz.

ACKNOWLEDGEMENTS

The authors would like to thank and gratefully acknowledge Universiti Malaysia Perlis for the financial support provided under the Fundamental Research Grant Scheme (FRGS) grant (FRGS/1/2019/TK04/UNIMAP/02/13). Special thanks to those who contributed to this project directly or indirectly.

REFERENCES

[1] H. Campanella, "Design and Modeling of Micro- and Nanoresonators," in Acoustic Wave and Electromechanical Resonators: Concept to Key Applications (Integrated Microsystems), Norwood, MA: Artech House, (2010) pp. 78-83.

[2] Y. Liu, Y. Cai, Y. Zhang, A. Tovstopyat, S. Liu, and C. Sun, Micromachines vol **11**, issue 7 (2020) pp. 630.

[3] R. Aigner and G. Fattinger, "3G - 4G - 5G: How BAW Filter Technology Enables a Connected World," in 20th International Conference on Solid-State Sensors, Actuators and Microsystems and Eurosensors *(*2019) pp. 523–526.

[4] M. Bousquet *et al.*, "Lithium Niobate Film Bulk Acoustic Wave Resonator for Sub-6 GHz Filters," in IEEE International Ultrasonics Symposium (2020) pp. 1-4.

[5] J. Wang, M. Park, S. Mertin, T. Pensala, F. Ayazi, and A. Ansari, Journal of Microelectromechanical Systems vol **29**, issue 5 (2020) pp. 741–747.

[6] M. H. Memon, Z. Khan, P. Zhang, H. Sun, and F. Lin, "Design of High-Q Film Bulk Acoustic Resonator for 5G Applications," in IEEE MTT-S International Wireless Symposium Proceedings (2020) pp. 1–3.

[7] N. Ashraf, Y. Mesbah, A. Emad, and H. Mostafa, "Enabling the 5G: Modelling and Design of High Q Film Bulk Acoustic Wave Resonator (FBAR) for High Frequency Applications," in IEEE International Symposium on Circuits and Systems (2020) pp. 1–4.

[8] M. H. Memon, Z. Khan, M. H. Memon, S. Chen, and F. Lin, "Film Bulk Acoustic Wave Resonator in RF Filters," in 15th International Computer Conference on Wavelet Active Media Technology and Information Processing, China, (2018) pp. 237–240.

[9] N. I. M. Nor, Y. W. Jing, and N. Khalid, "Characteristics of Film Bulk Acoustic Wave Resonator Using Different Electrode Materials," in AIP Conference Proceedings, Malaysia, (2021) pp. 20144.

[10] I. S. Uzunov, M. D. Terzieva, B. M. Nikolova, and D. G. Gaydazhiey, "Extraction of Modified Butterworth — Van Dyke Model of FBAR based on FEM Analysis," in XXVI International Scientific Conference Electronics, Bulgaria, (2017) pp. 1–4.